Evaluating Intramolecular Hydrogen Bond Strengths in (1−4) Linked Disaccharides from Electron Density Relationships

Jeff Yu-Jen Chen and Kevin J. Naidoo*

Department of Chemistry, University of Cape Town, Rondebosch 7701, South Africa

Received: June 4, 2003

The binding energy of intermolecular hydrogen bonds can be readily and accurately assessed using model pairs of functional groups; however, the energy of intramolecular hydrogen bonds as found in carbohydrates and folded proteins has not been computationally and experimentally accessible. We present a procedure to evaluate the intramolecular hydrogen bond strength from a set of correlation curves based on the electron density within the hydrogen bond. B3LYP 6-31G(d), 6-31+G(d,p), and 6-311++G(d,p) were used to optimize all combinations of functional group OH, NH_2, and $NHCOCH_3$ pairs. The intermolecular hydrogen bonds and the electron density in the hydrogen bond were measured using Bader's atoms in molecules method. A linear relationship between the binding energy/hydrogen bond strength (ΔE^{HB}) and a modified Grabowski complex parameter (Δ_{el+lap}) for the entire set of functional group pairs was established. Correlation curves (ΔE^{HB} vs Δ_{el+lap}) for each individual pair of functional groups were then constructed by measuring the electron density (using Bader's atoms in molecules method) and the intermolecular binding energy as the hydrogen bond is compressed and extended. This ΔE^{HB} vs Δ_{el+lap} curve was then used to estimate the intramolecular cross glycosidic hydrogen bond strength of 1−4 linked disaccharides by calculating Δ_{el+lap} for the minima conformation. On the basis of these data, the hydrogen bond strengths between functional groups located across the glycosidic linkage from each other were evaluated and then ranked from the strongest (viz., $NHCOCH_3$(D)···NH_2(A)) to the weakest (viz., NH_2(D)···NH_2(A)).

Introduction

Hydrogen bonding is the cornerstone of macromolecular secondary and tertiary structure. There are two classes of hydrogen bonds that determine the conformation and intermolecular interactions of biomolecules in solution. These are the internal or *intramolecular* hydrogen bonds that often compete with the external solute to solvent *intermolecular* hydrogen bonds in a biomolecular folding environment. In the case of globular proteins 90% of the hydrogen bonds are due to the interactions between the main chain N−H and main chain C═O groups forming secondary structure (α-helices, *β*-sheets, etc.).[1] The majority of intramolecular hydrogen bonds in polysaccharides take place between small functional groups (e.g., hydroxyls, amines, and acetylamides) branching off pyranose or furanose rings that are in close proximity to each other. More important are the hydrogen bonds that form across glycosidic linkages joining adjacent sugar rings along a saccharide chain. These account for the macromolecular structure of polysaccharides[2] and the structural specificity, of oligosaccharides found in glycoproteins, required for molecular recognition in cell−cell interactions.[3]

There have been some experimental[4] and ab initio[5−8] investigations into the nature of the hydrogen bond between functional groups of biological relevance. At the same time molecular mechanics studies often invoke hydrogen bond explanations to rationalize conformational and binding observations.[9] The overall topology of a large polysaccharide is influenced significantly by the performance of the individual glycosidic dihedral angles in the polymer. Here the strength of the cross-glycosidic intramolecular hydrogen bond has a significant effect on the degree of rotational flexibility of the glycosidic dihedral angles. However, within the condensed medium, this intramolecular hydrogen bond is in competition with water molecules that form hydrogen-bonded bridges between residues across the linkages.[10] The introduction of a bridging intermolecular-bonded water molecule that is in regular exchange with the intramolecular cross glycosidic linkage hydrogen bonds will significantly affect the conformation and properties of an oligosaccharide. One possible means of controlling the strength of a polysaccharide material would be to prevent the occurrence of such phenomenon through increasing the strength of the intramolecular hydrogen bonds across the glycosidic linkage so as to exclude the intermolecular hydrogen bonds formed with the bridging water.[11]

In general it is not possible to accurately estimate the strength of an intramolecular hydrogen bond from ab initio calculations. As a result there has to date not been a systematic attempt to rank the hydrogen bond strength across the glycosidic linkage apart from our preliminary studies.[12] In the meantime there have been many theoretical investigations into intermolecular hydrogen bonding in small organic molecules. Most studies, on medium-sized molecules of the type we are interested in, employed the Hartee−Fock (HF) level of theory. Hydrogen bond strengths between pairs of functional groups such as hydroxyls and amines are determined from intermolecular binding energies. It is possible to approach the HF limit of the binding energy using a sufficiently large basis set, and in some cases these energies are in agreement with experimental binding energies. This, however, is due to a fortuitous cancellation of errors stemming from limitations in the basis set and the wave

* To whom correspondence should be addressed. E-mail: knaidoo@science.uct.ac.za. Fax: +27-21-689-7499.

10.1021/jp035574f CCC: $25.00
Published on Web 08/06/2003

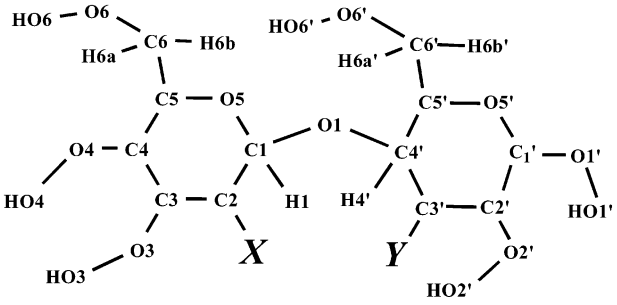

	-X	-Y
Φ = H1 - C1 - O1 - C4'	-OH	-OH
	$-NH_2$	-OH
ψ = C1 - O1 - C4' - H4'	$-NH_2$	$-NH_2$
	$-NHCOCH_3$	-OH
	$-NHCOCH_3$	$-NH_2$
	$-NHCOCH_3$	$-NHCOCH_3$
	$-OCH_3$	$-OCH_3$
	$-OCH_3$	-OH
	$-CH_3$	$-CH_3$

Figure 1. Atomic, dihedral angle, and functional group labels for the $\beta(1-4)$ disaccharides and their derivatives. The same labels apply to the $\alpha(1-4)$ analogues.

function models. Moreover, a more serious criticism of the HF method is its neglect of electron correlation, which results in an overestimation in bond lengths.[13] Density functional theory (DFT) based methods, such as the Becke−three Lee−Yang−Parr (B3LYP)[14] one, have been shown to provide reliable trends of binding energies even though the small energy differences often observed in relative binding energies can be overshadowed by the DFT quadrature errors.[13] This weakness can be overcome by increasing the basis set size, as has been recommended by Gálvez et al. that the B3LYP/6-311++G(d,p) is the preferred method for calculating hydrogen bond strengths.[15]

Our main objective here is to rank the hydrogen bond strength of various combinations of the following functional groups: OH, NH_2, and $NHCOCH_3$ as they are found in 1−4 linked saccharides and illustrated in Figure 1. We are able to achieve this objective and arrive at a ranking of intramolecular hydrogen bonds by quantifying the relationship between hydrogen bond strength and electron density within the hydrogen bonds occurring between pairs of functional groups.

Hydrogen Bonding Theory

The common expression for estimating hydrogen bond strengths between a hydrogen donor molecule (D) and the molecule accepting the hydrogen (A) is to divide the energy of the molecular pair into a contribution from the two molecules plus the overall lower interaction energy such that

$$\Delta E^{HB} = E(D-H\cdots A) - [E(D-H) + E(A)] \qquad (1)$$

Decomposing the interaction energy (ΔE^{HB}) into electrostatic and quantum mechanical components is somewhat artificial in terms of molecular orbital theory; however, this approach has been used to facilitate a chemical understanding of the makeup of hydrogen bonds. This decomposition of ΔE^{HB} can be investigated using the framework of perturbation theory.[16] In perturbation theory the contribution to the self-consistent field (SCF) interaction energy (ΔE^{Def}_{SCF}) is associated with the deformation of the zeroth-order perturbation wave functions of the hydrogen donor (Ψ^0_D) and the hydrogen acceptor (Ψ^0_A) molecules, which results from the interaction between the electrons and the nuclei on the two different molecules. The interaction operator ($\hat{V}$) acts on the relaxed, fully symmetrized SCF wave function of the hydrogen-bonded complex ($\Psi_{D,A}$), giving the deformation energy

$$\Delta E^{Def}_{SCF} = \langle \Psi_{D,A}|\hat{V}|\Psi_{D,A}\rangle - (ES + EX) \qquad (2)$$

which is equivalent to ΔE^{HB}. The second term in eq 2 is the combined electrostatic energy (ES) and the quantum mechanical exchange energy (EX) arising from the antisymmetry operator ($\hat{A}$) acting on the zeroth-order perturbation wave functions, i.e.,

$$\langle \hat{A}\Psi^0_D\Psi^0_A|\hat{V}|\hat{A}\Psi^0_D\Psi^0_A\rangle \qquad (3)$$

Morokuma developed a decomposition method[17] that subpartitioned the total Hartree−Fock (HF) derived binding energy (ΔE^{Def}_{SCF}) into electrostatic, polarization, exchange repulsion, charge transfer, and coupling components. Using procedures of this type it has become widely accepted that energetically moderate hydrogen bonds involved in biomolecular systems (e.g., proteins, polysaccharides, nucleic acids, etc.) are principally electrostatic in nature. However, this procedure is flawed because differentiating the orbital space between the above terms is largely arbitrary[16,18] and so it is not possible to distinguish between the charge transfer and polarization terms.[19] Furthermore, the lack of electron correlation at the Hartree−Fock level of theory makes the response of electrons in one part of the hydrogen-bonded system to the positions of electrons in another part less accurate.

A more direct approach to assessing the quantum mechanical nature of the hydrogen bond is to calculate directly the relation between electron density and hydrogen bond strength. The problem is to define the electron density in the volume between the D and A participants in the hydrogen bond. The overall electron density can be calculated from the wave function of the hydrogen-bonded complex over all *N* atomic coordinates.

$$\rho(\vec{r}_{D-H---A}) = \int |\Psi_{D,A}(\vec{r}_1,\vec{r}_2,...,\vec{r}_N)|^2 \, d\vec{r}_1,d\vec{r}_2,...,d\vec{r}_N \qquad (4)$$

An absolute electron density ($\rho(r)$) associated with the hydrogen bond, that is comparable for all combinations of functional groups capable of hydrogen bonding, is best calculated using Bader's atoms in molecules (AIM) theory.[20] The electron density may be analyzed in terms of its topology (maxima, minima, and saddle points) by partitioning the molecules into atomic basins. A gradient vector map ($\nabla\rho(\hat{r})$) is generated and an *interatomic surface* (a surface that separates the atomic basins of neighboring atoms) can then be analyzed. The bond path is then the line through space between D−H and A along which the electron density is a maximum whereas the point of lowest $\rho(r)$ on this line is the *bond critical point* (BCP). There are two sets of trajectories associated with the BCP, (1) the set that terminates at the critical point and defines the interatomic surface and (2) the pair that originates at the critical point and defines the line of maximum density.[21] An accurate estimate of the strength a hydrogen bond can be determined when the electron density distribution satisfies eight topological criteria and the hydrogen atom complies with four properties. These have been derived in detail by Koch and Popelier[22] and conveniently summarized in a paper by Pacios and Gómez.[8] The major advantages of the AIM method are its

ability to produce system independent robust results and that the method is not highly basis set dependent.[20]

Although intermolecular hydrogen bond energies between independent (i.e., not bonded) functional groups can be estimated by calculating the binding energy between two molecules, an accurate measure of intramolecular hydrogen bond strengths for multifunctional molecules is not available. Estimates of the energy of intramolecular hydrogen bonds have been achieved by taking the difference in energy of the maximally oriented hydrogen-bonded configuration, i.e., E(D−H···A) and the energy of an anti-hydrogen-bonded configuration that has the D−H proton-donating bond rotated away from the acceptor atom (A) by 180°, i.e., E(H−D···A).[23,24] The difference in energy between these two configurations does not correctly reveal the energy of the hydrogen bond (ΔE^{HB})[24] because strain effects and electronic steric repulsions are embedded in these energy differences. Moreover, procedures of this kind are not suitable for molecules with multiple hydrogen bonds found in close proximity to each other, as is the case in disaccharides. Rotating a single hydrogen bond, in the way described above, in the presence of a set of adjacent hydrogen bonds will result in an energy difference between the conformations that is artificially higher than the energy resulting from only the electrostatic and electronic contributions to hydrogen bonding. Grabowski proposed that the hydrogen bond strength may be adequately described on the basis of either the geometrical data, the topological parameters, or the Laplacian values of the electron densities exhibited by the hydrogen-bonded complex.[25] By combining these three factors a complex parameter ($\Delta_{geo+el+lap}$) was developed and shown to have a linear relationship with the hydrogen bond energy.[25] We find that it is sufficient to include only the electron density in the hydrogen bond and the Laplacian of the electron density to achieve a strong linear relationship with hydrogen bond strength. In this modified Grabowski complex parameter shown in eq 5 the ρ_{BCP} and $\nabla^2\rho_{BCP}$ correspond to the electron density and Laplacian of the electron density of a proton donor bond (D−H) involved in hydrogen bonding. The ρ^0_{BCP} and $\nabla^2\rho^0_{BCP}$ correspond to the electron density and Laplacian of the electron density of bond (X−H) not involved in hydrogen bonding.

$$\Delta_{el+lap} = \frac{(\rho^0_{BCP} - \rho_{BCP})}{\rho^0_{BCP}} + \frac{(\nabla^2\rho^0_{BCP} - \nabla^2\rho_{BCP})}{\nabla^2\rho^0_{BCP}} \qquad (5)$$

Here we develop correlation curves between hydrogen bond strengths (ΔE^{HB}) and a modified Grabowski's complex parameter (Δ_{el+lap}) from all hydrogen donor and acceptor combinations of the following functional groups: OH, NH_2, and $NHCOCH_3$) by varying distances between D and A. These ΔE^{HB} vs Δ_{el+lap} correlation curves are used to estimate the ΔE^{HB} value for the cross glycosidic intramolecular hydrogen bond by calculating the Δ_{el+lap} parameter for the minima conformation of each of the 1−4 linked disaccharide derivatives (as shown in Figure 1).

Computational Details

Full geometry optimization was performed under the restricted closed shell ground electronic state for all the pairs of functional groups using Gaussian 98.[26] All geometry optimizations of the pairs of functional groups were performed using the Becke−three Lee−Yang−Parr (B3LYP)[14] density functional method. Three different levels of basis sets, 6-31G(d), 6-31+G(d,p), and 6-311++G(d,p), were used in the optimization of the functional group pairs. Due to the shallow potential curves of these systems, the keyword OPT=Tight was included to increase the convergence criteria. This ensures a better reliability of the final geometries. For each optimization, vibrational frequency calculations were carried out to confirm that the global minimum state was reached for each pair of molecules. It was necessary to calculate all the donor−acceptor orientations to allow us to estimate the magnitude of the hydrogen bonds as observed in the disaccharides. As a result we optimized Me−NH_2(D)- - -Me−OH(A) and Me−NAc(D(H))- - -Me−NAc(A(N)) (amide hydrogen of the first NAc group as hydrogen bond donor and amide nitrogen of the second NAc group as the hydrogen acceptor) for which a single imaginary frequency was observed. This is explicable because it was previously shown that oxygen is a superior hydrogen bond donor compared with nitrogen, and so locating the global minimum state when nitrogen is the hydrogen bond donor is a near impossiblity.[27] All other functional group pairs reached the global minima on optimization.

Binding energy evaluations were performed with a Boys−Benardi functional counterpoise scheme.[28] The standardized ΔE^{HB} vs Δ_{el+lap} correlation curves were constructed by using the restricted closed shell electronic ground-state B3LYP method with the 6-311++G(d,p) basis set for all functional group pairs including both Me−NH_2(D)- - -Me−OH(A) and Me−NAc-(D(H))- - -Me−NAc(A(N)).

The disaccharides were optimized with B3LYP/6-31G(d) initially. After the the results were examined, only selective disaccharides with the lowest energy conformation were optimized with the B3LYP/6-311++G(d,p) basis set. The topological properties of the electronic density were characterized using the AIM methodology[20] for all the calculations as implemented in Gaussian 98[26] and AIM2000.[29]

Results and Discussion

We have calculated the binding energies of all combinations of the following functional groups: Me−CH_3, Me−OCH_3, Me−NH_2, Me−OH, and *trans*-Me−N(H)−C(=O)−CH_3 (Me−*N*-acetylamide, Me−NAc). Alkylamides show planar symmetry as the electrons are delocalized along the amide bond therefore exhibiting partial double bond character. Two distinct species of geometric isomers can be found for any of the alkylamides. The trans *N*-alkyl isomer is highly preferred over the cis isomer regardless of the solvation medium.[30] Consequently, only hydrogen bonding involving the trans Me−NAc group have been investigated here.

There have been many ab initio studies on the various hydrogen-bonded complexes involving the functional groups, Me−OH, Me−NH_2, and Me−NAc.[6,7,31−34] Early ab initio work for the methanol dimer was pioneered by Del Bene[31] followed by numerous HF calculations differing only in the level of basis set used. Dixon et al. performed a HF/6-31G(d) calculation on a methanol dimer complex[32] and found a binding energy of −4.10 kcal/mol, which is within the range of −3.2 to −4.1 kcal/mol limit measured from experiments.[35] These calculations did not include a correction for basis set superposition error (BSSE) and electron correlation; therefore the comparison with experimental energies and geometries are predictably poor. When BSSE were corrected for and electron correlation was included as in the Hagemeister et al. B3LYP/6-31+G(2d,p) zero point energy (ZPE) level calculations,[34] the resulting binding energies were comparable to the experimental values.

To date, one of the most comprehensive computational studies on moderate hydrogen bonds of biomolecular significance has been that of Kim and Freisner.[6] The objective of this study was

TABLE 1: Hydrogen-Bonded Functional Pairs that Have Been Optimized and Evaluated with Three Different Methods, (I) B3LYP/6-31G(d), (II) B3LYP/6-31+G(d,p), and (III) B3LYP/6-311++G(d,p), Ranked from Strongest to Weakest Hydrogen Bond

rank	donor	acceptor	I ΔE^{HB} (kcal/mol)	II ΔE^{HB} (kcal/mol)	III ΔE^{HB} (kcal/mol)	A···D dist (Å)	H···D dist (Å)	A−H···D angle (deg)
1	Me−OH	Me−NH2	−7.707	−7.348	−7.091	1.900	2.878	172.48
2	Me−OH	Me−NAc	−6.714	−6.840	−6.527	1.873	2.833	168.42
3	Me−NAc	Me−NH2	−6.311	−6.235	−6.123	2.118	3.136	175.61
4	Me−NAc	Me−NAc	−5.647	−5.882	−6.086	1.999	3.007	172.72
5	Me−OH	Me−OCH3	−4.865	−5.333	−5.273	1.887	2.858	178.58
6	Me−OH	Me−OH	−4.665	−5.037	−5.163	1.905	2.873	176.00
7	Me−NAc	Me−OH	−4.812	−4.832	−4.864	2.001	3.020	175.96
8	Me−NH_2	Me−NAc	−4.251	−3.858	−3.765	2.162	3.136	159.58
9	Me−NH_2	Me−NH2	−3.896	−3.263	−2.898	2.261	2.261	169.03
10[a]	Me−NH_2	Me−OH	−2.438	−2.551	−2.625	2.159	3.106	154.26
11[b]	Me−OCH_3	Me−OCH3	−0.777	−1.119	−1.569	3.601	2.769	132.58
12[c]	Me−NAc	Me−NAc	−1.337	−1.126	−1.051	2.452	3.426	−161.51
13	Me−CH_3	Me−CH3	−0.008	−0.005	−0.002			

[a] Conformation with 1 imaginary frequency (transitional state). [b] Improper hydrogen bond. [c] Conformation with 1 imaginary frequency (transitional state) where the amide hydrogen of one of the NAc groups is pointing toward nitrogen on the adjacent NAc group.

to provide a resource for developers of molecular mechanics protein force fields. They optimized the dimer geometries with HF/6-31G** followed by MP2/cc-pVTZ(-f/d) energy evaluations. We optimized pairs of functional groups with basis sets (I) B3LYP/6-31G(d), (II) B3LYP/6-31+G(d,p), and (III) B3LYP/6-311++G(d,p) and compared the geometries and binding energies with published DFT and MP2 data[6,7,31−34,36] where possible. On the whole the B3LYP results are in agreement with the MP2 ones. The relative hydrogen bond strengths for the functional group pairs derived from B3LYP counterpoise corrected binding energies are shown in Table 1. Of particular note is the result predicting the Me−OH(D)- - -Me−NH_2(A) hydrogen bond to be more than 3.5 kcal/mol stronger than the Me−NH_2(D)- - -Me−OH(A). This is consistent with previous studies that show hydroxyls to be better hydrogen bond donors than amines.[6]

Electron Density Hydrogen Bond Correlation Curves. We use the AIM procedure to analyze the electron density in the hydrogen bonds of the pairs of functional groups listed in Table 1. Except for the methylated dimers, all of the hydrogen-bonded pairs comply with the criterion required for hydrogen bonding summarized by Pacios and Gómez.[8] It has been suggested by Cheeseman et al. that the near-perfect transferability of electron density of atoms does contribute to the total energy.[37] On the basis of this postulation and supported by the results of Grabowski,[25] we construct the standardized correlation curves by plotting the binding energies of the fully optimized complexes (ΔE^{HB}) evaluated from B3LYP/6-311++G(d,p)//B3LYP/6-311++G(d,p) against the modified Grabowski parameter Δ_{el+lap}. The results of a survey of crystal structures showed that the directionality of hydrogen bonds were consistent with the diffusive nature and the directional properties of the lone-pair electron densities of acceptors atoms.[38] Furthermore, the effect of the D−H- - -A angle on the binding energy of the Me−NAc hydrogen-bonded dimer has been investigated using AM1 semiempirical methods. The results showed a very minor correlation between the variation in angle and the hydrogen bond energy.[39] Therefore, though hydrogen bonds are directional and the overall range of the D−H- - -A angle is limited between 180° and 140°, for a medium to strong hydrogen bond, the distance between the hydrogen donor and acceptor atoms makes the most significant contribution to the strength of the hydrogen bond. This being the case we kept the D−H- - -A angle fixed at the value obtained from the optimized geometry (generally not smaller than 155°) and varied the distance between D and A from a minimum distance where the van der Waals radii of the acceptor atom and the donor hydrogen are in contact to a maximum distance where the electron density is zero for each of the fully optimized combinations of functional donor−acceptor pairs. The modified Grabowski parameter and binding energy were calculated for each D and A distance and so a binding energy−Δ_{el+lap} correlation was established for each functional group pair. The Δ_{el+lap} versus the binding energy correlation curves for all the hydrogen donor−acceptor pairs are shown in Figure 2. The parabolic nature of these curves allows for comparison between the interacting pairs. It is clear that the electron density in the hydrogen bond is a strong indicator of the hydrogen bond strength, which implies that electron delocalization, as in an actual chemical bond, is a significant contributor to the character of hydrogen bonds.[40]

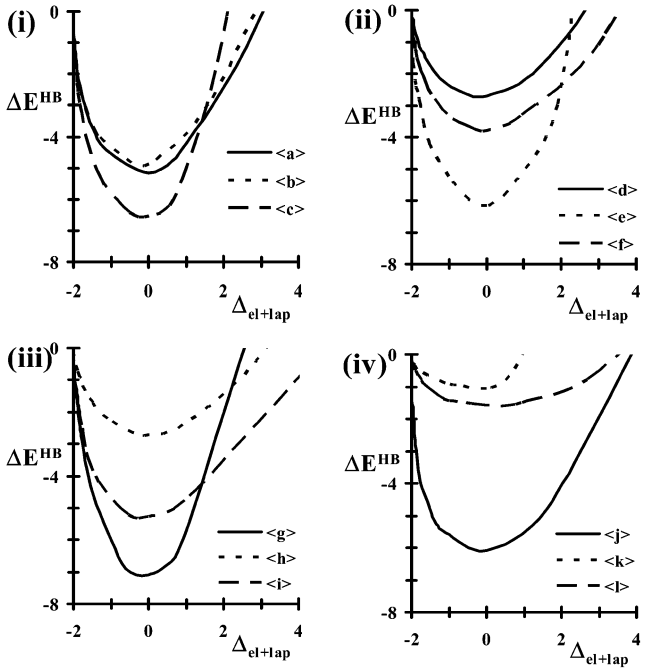

Figure 2. Correlation Δ^{HB} vs Δ_{el+lap} curves constructed using a B3LYP/6-311++G(d,p) basis set: (i) ⟨a⟩ Me−OH- - -Me−OH, ⟨b⟩ Me−OH-(D)- - -Me−NAc(A), ⟨c⟩ Me−OH(A)- - -Me−NAc(D), (ii) ⟨d⟩ Me−NH_2- - -Me−NH_2, ⟨e⟩ Me−NAc(D)- - -Me−NH_2(A), ⟨f⟩ Me−NAc(A)−Me−NH_2(D), (iii) ⟨g⟩ Me−NH_2(A)- - -Me−OH(D), ⟨h⟩ Me−NH_2(D)- - -Me−OH(A)†, ⟨i⟩ Me−OH(D)- - -Me−OCH_3(A) (iv) ⟨j⟩ Me−NAc- - -Me−NAc, ⟨k⟩ Me−NAc- - -Me−NAc‡, and ⟨l⟩ Me−OCH_3- - -Me−OCH_3.

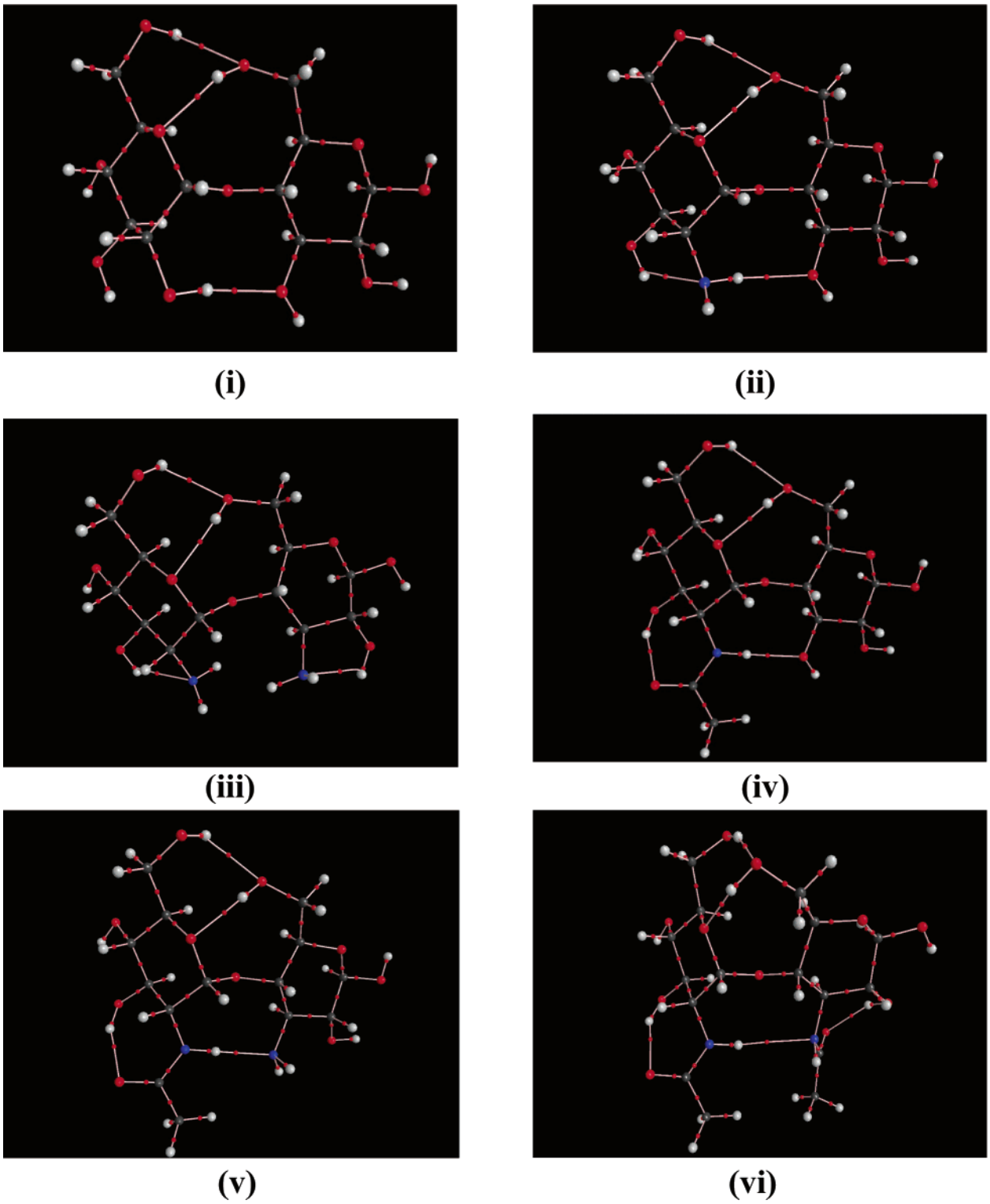

Figure 3. Molecular graphs of the B3LPY/6-311++G(d,p) optimized α(1−4) disaccharides where the small red spheres indicate the positions of the BCPs. The disaccharides shown are (i) maltose, (ii) α-D-Glc-2-NH_2-(1→4)-*β*-D-Glc, (iii) α-D-Glc-2-NH_2-(1→4)-*β*-D-Glc-3-NH_2, (iv) α-D-Glc-2-NAc−(1→4)-*β*-D-Glc, (v) α-D-Glc-2-NAc−(1→4)-*β*-D-Glc-3-NH_2, and (vi) α-D-Glc-2-NAc−(1→4)-*β*-D-Glc-3-NAc.

Intramolecular Hydrogen Bonding: Disaccharides. The binding energy of intermolecular hydrogen bonds can be readily and accurately assessed using model pairs of functional groups such as the ones analyzed in the previous section. However, it is nearly impossible to tease out the contribution of individual intramolecular hydrogen bonds to the internal energy of a macromolecule because electrostatic, steric, and electronic effects are always present. It is here that the predictive value of the correlation ΔE^{HB} vs Δ_{el+lap} curves shown in Figure 2 can be demonstrated. We investigate the strength of hydrogen bonds across glycosidic linkages for both α and *β*(1−4) linked disaccharides, as illustrated in Figure 1 using the correlation curves of Figure 2.

The conformations of oligosaccharides are dictated by the flexibility of the glycosidic linkages and in turn the hydrogen bonds formed across those linkages. We have previously

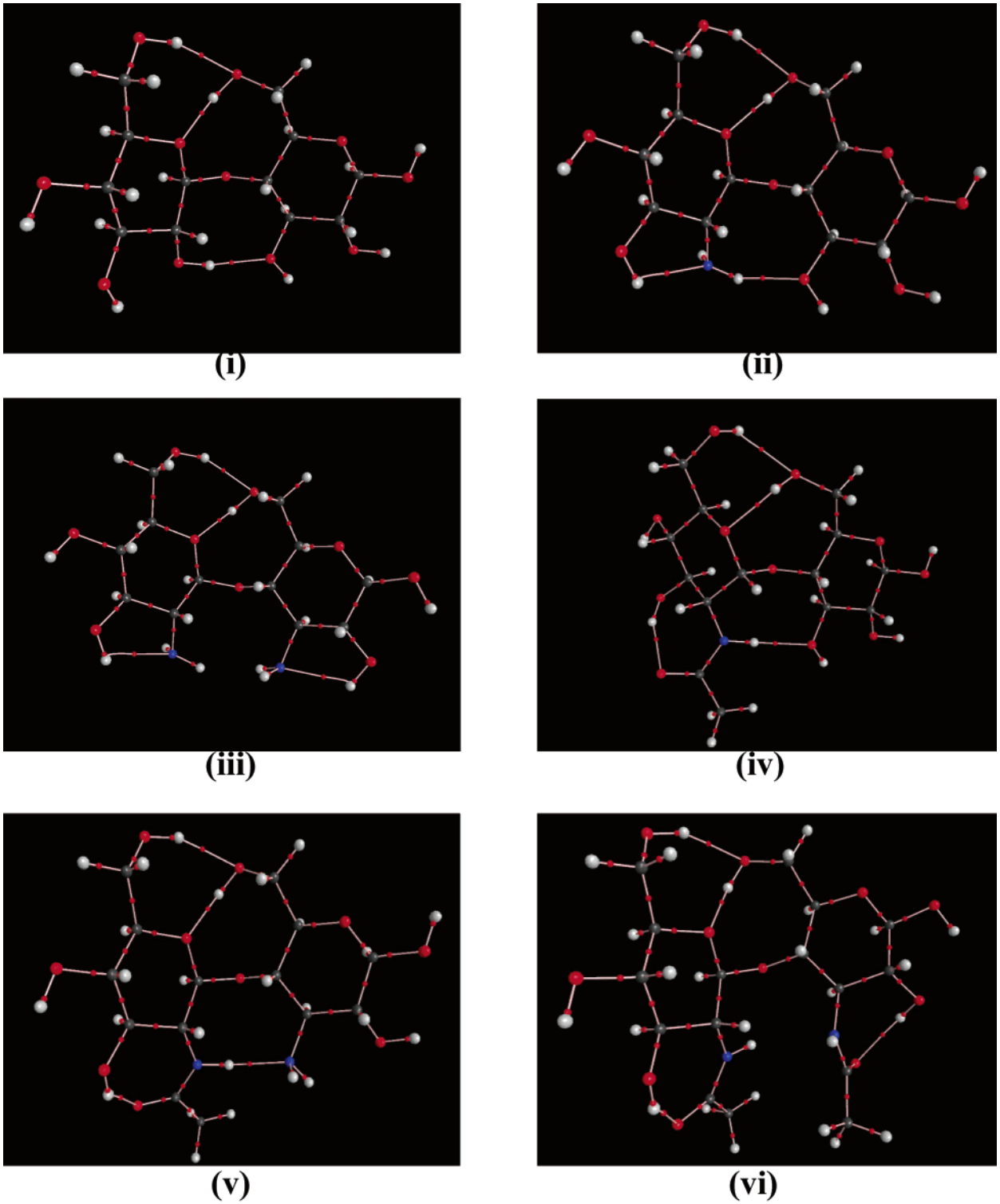

Figure 4. Molecular graphs of the B3LPY/6-311++G(d,p) optimized $\beta(1-4)$ disaccharides where the small red spheres indicate the positions of the BCPs. The disaccharides shown are (i) cellobiose, (ii) β -D-Glc-2-NH_2-(1→4)-β-D-Glc, (iii) β-D-Glc-2-NH_2-(1→4)-β-D-Glc-3-NH_2, (iv) β-D-Glc-2-NAc−(1→4)-β-D-Glc, (v) β-D-Glc-2-NAc−(1→4)-β-D-Glc-3-NH_2, and (vi) β-D-Glc-2-NAc−(1→4)-β-D-Glc-3-NAc.

investigated the nature of the $\alpha(1-4)$ and $\alpha(1-6)$ linkages[41] and found that the flexibility of the $\alpha(1-4)$ linkage in solution is affected by the extent of rapid exchange between bridging intermolecular water hydrogen bonds, formed with the hydroxyls at C2 and C3′, and the intramolecular hydrogen bonds usually found between these hydroxyls in the solid state.[10,11] Preliminary investigation into derivatives of $\alpha(1-4)$ linked saccharides was done with a view to the slowing down this exchange of intermolecular and intramolecular hydrogen bonds through increasing the intramolecular hydrogen bond strength by substituting functional groups of varied hydrogen bond accepting and donating properties at the C2 and C3′ positions (Figure 1).[12]

B3LYP/6-31G(d) optimizations were carried out on all the disaccharide combinations listed in Figure 1. Combinations of clockwise and anticlockwise hydroxyl orientations on the reducing and nonreducing sugars were optimized and compared as a way to identify conformations with the lowest energies. The low-energy conformations for each of the disaccharides

TABLE 2: Geometry Parameters and the Estimation of H-Bond Strength (ΔE^{HB}) of the B3LYP/6-311++G(d,p) Optimized Disaccharides

rank	−X	−Y	estimated ΔE^{HB} [a] (kcal/mol)	ϕ	Ψ	H- - -A dist (Å) C3−C2	C2−C3′	C3′−C2′
				α(1−4) linked				
1	−NAc	$-NH_2$	−6.03	−14.08	1.55	1.845	1.957	2.475
2	$-OCH_3$	−OH	−5.01	−8.59	3.00	2.469	1.964	2.287
3	−OH	−OH	−4.99	−6.80	7.11	2.358	1.922	2.360
4	−NAc	−OH	−4.76	−13.80	2.77	1.856	1.945	2.286
5	$-NH_2$	−OH	−2.51	−9.79	6.53	2.220	2.127	2.308
6	$-OCH_3$	$-OCH_3$	−1.01	−12.59	2.20	2.302	2.669	2.891
7	−NAc	−NAc	−0.97	−24.86	−38.86	1.941	2.660	2.001
8	$-NH_2$	$-NH_2$	N/A	−24.91	−12.00	2.246	N/A	2.267
9	$-CH_3$	$-CH_3$	N/A	−25.53	−10.39	N/A	N/A	N/A
				β(1−4) linked				
1	−NAc	$-NH_2$	−6.08	176.27	7.83	1.760	1.963	2.487
2	−OH	−OH	−5.02	180.93	0.79	2.366	1.889	2.307
3	$-OCH_3$	−OH	−4.89	187.21	7.83	2.366	1.893	2.603
4	−NAc	−OH	−4.62	176.66	8.17	1.767	1.945	2.262
5	$-NH_2$	−OH	−2.47	176.18	2.87	2.785	2.081	2.274
6	$-OCH_3$	$-OCH_3$	−0.98	160.20	4.13	2.451	N/A	3.126
7	$-NH_2$	$-NH_2$	N/A	188.07	12.40	2.404	2.210	2.195
8	−NAc	−NAc	N/A	166.76	6.01	1.743	N/A	2.051
9	$-CH_3$	$-CH_3$	N/A	162.17	9.62	N/A	N/A	N/A

[a] For cross-glycosidic linkage only.

were further optimized with B3LYP/6-311++G(d,p) and the resultant electron density analyzed using AIM calculations. The molecular graphs of six global minimum geometry α(1−4) linked disaccharides (maltose, α-D-Glc-2-NH_2-(1→4)-β-D-Glc, α-D-Glc-2-NH_2-(1→4)-β-D-Glc-3-NH_2, α-D-Glc-2-NAc−(1→4)-β-D-Glc, α-D-Glc-2-NAc−(1→4)-β-D-Glc-3-NH_2 and α-D-Glc-2-NAc−(1→4)-β-D-Glc-3-NAc) are displayed in Figure 3i−vi, respectively. Similarly, the corresponding six β(1−4) linked disaccharides (cellobiose, β-D-Glc-2-NH_2-(1→4)-β-D-Glc, β-D-Glc-2-NH_2-(1→4)-β-D-Glc-3-NH_2, β-D-Glc-2-NAc−(1→4)-β-D-Glc, β-D-Glc-2-NAc−(1→4)-β-D-Glc-3-NH_2 and β-D-Glc-2-NAc−(1→4)-β-D-Glc-3-NAc) are shown in Figure 4i−vi, respectively.

Interglycosidic hydrogen bonds between the hydroxyl groups on C2 and C3′ are present in both maltose and cellobiose. Estimating the hydrogen bond strength using the ΔE^{HB} vs Δ_{el+lap} correlation curves gives a value of approximately 5 kcal/mol. Interestingly, the intramolecular interaction between the vicinal hydroxyl groups located on the C3 and C2 as well as the C3′ and C2′ do not satisfy the AIMs criterion for hydrogen bonding. This result confirms the previous observation for 1−2-diols[42] because there is no electron density between these adjacent hydroxyl functional groups.

Ranking the intramolecular hydrogen bond strengths of the (1−4) linked disaccharides derivatives with functional groups substituted at the C2 (X) and C3′ (Y) positions (Table 2) produced a different trend than that of the corresponding intermolecular hydrogen bonds listed Table 1. The strongest intermolecular hydrogen bond is Me−NH_2(A)- - -Me−OH(D), which is not the case with this functional group pair substituted about the glycosidic α and β(1−4) linkage. Rather, the functional groups exhibiting the strongest hydrogen bond across both α and β(1−4) glycosidic linkages are the NAc(D)- - -NH_2-(A) combination. The reason for the differences in the two trends lies with the formation of strong intramolecular hydrogen bonds between the hydroxyls and the adjacent NH_2 groups on the nonreducing sugar of α- and β-D-Glc-2-NH_2-(1→4)-β-D-Glc; this results in the amine being orientated to form a weak cross glycosidic linkage hydrogen bond (NH_2(D)- - -OH(A)) with the hydroxyl group on C(3)′ on the reducing sugar (see Figures 3ii and 4ii). In contrast, the hydroxyls on the nonreducing sugars of α- and β-D-Glc-2-NAc−(1→4)-β-D-Glc-3-NH_2 form strong intramolecular hydrogen bonds with the NAc groups on the nonreducing sugar, which results in the NAc being directed to form a strong cross glycosidic hydrogen bond with the amine on the reducing sugar (see Figures 3v and 4v). An examination of the electron density maps in Figure 5, (a) α-D-Glc-2-NAc−(1→4)-β-D-Glc-3-NH_2 and (b) β-D-Glc-2-NAc−(1→4)-β-D-Glc-3-NH_2, confirms the existence of hydrogen bonding between these vicinal groups, as seen in the molecular graphs of Figures 3v and 4v. Unlike the vicinal hydroxyl groups on the reducing and nonreducing sugars of maltose and cellobiose that do not exhibit hydrogen bonding, BCPs do occur between the hydroxyls and the NAcs of the nonreducing sugar for both α and β linkages (Figure 5i,iv) with the correct topology for hydrogen bonding. These hydrogen bonds between the vicinal groups on the nonreducing sugar rings optimally direct the NAc toward the amine, inducing a strong hydrogen bond of approximately 6 kcal/mol for both α and β derivatives compared to approximately 5 kcal/mol for the equivalent cross glycosidic hydrogen bond found in maltose and cellobiose.

Although the Me−NAc- - -Me−NAc dimer complex produced a relatively strong intermolecular hydrogen bond when both X and Y sugar positions were substituted with NAc groups, significant steric repulsion between these bulky groups occurs. Consequently, no BCP was found between substituents in α-D-Glc-2-NAc−(1→4)-β-D-Glc-3-NAc, resulting in only a weak cross-glycosidic electrostatic attraction. The β-D-Glc-2-NAc−(1→4)-β-D-Glc-3-NAc disaccharide produced a very weak hydrogen bond between the amide hydrogen of the nonreducing sugar and the amide nitrogen of the reducing sugar.

Conclusion

Evaluating relative intramolecular hydrogen bond strengths in folded saccharides and other biopolymers is an important component in the rational design of conformationally dependent "lock and key" binding. The contributions of intramolecular hydrogen bonds to the conformational energy of biopolymers have previously not been accessible, as that energetic contribution had been buried in a large mix of electrostatic, van der Waals, and quantum terms. Only a rough approximation could

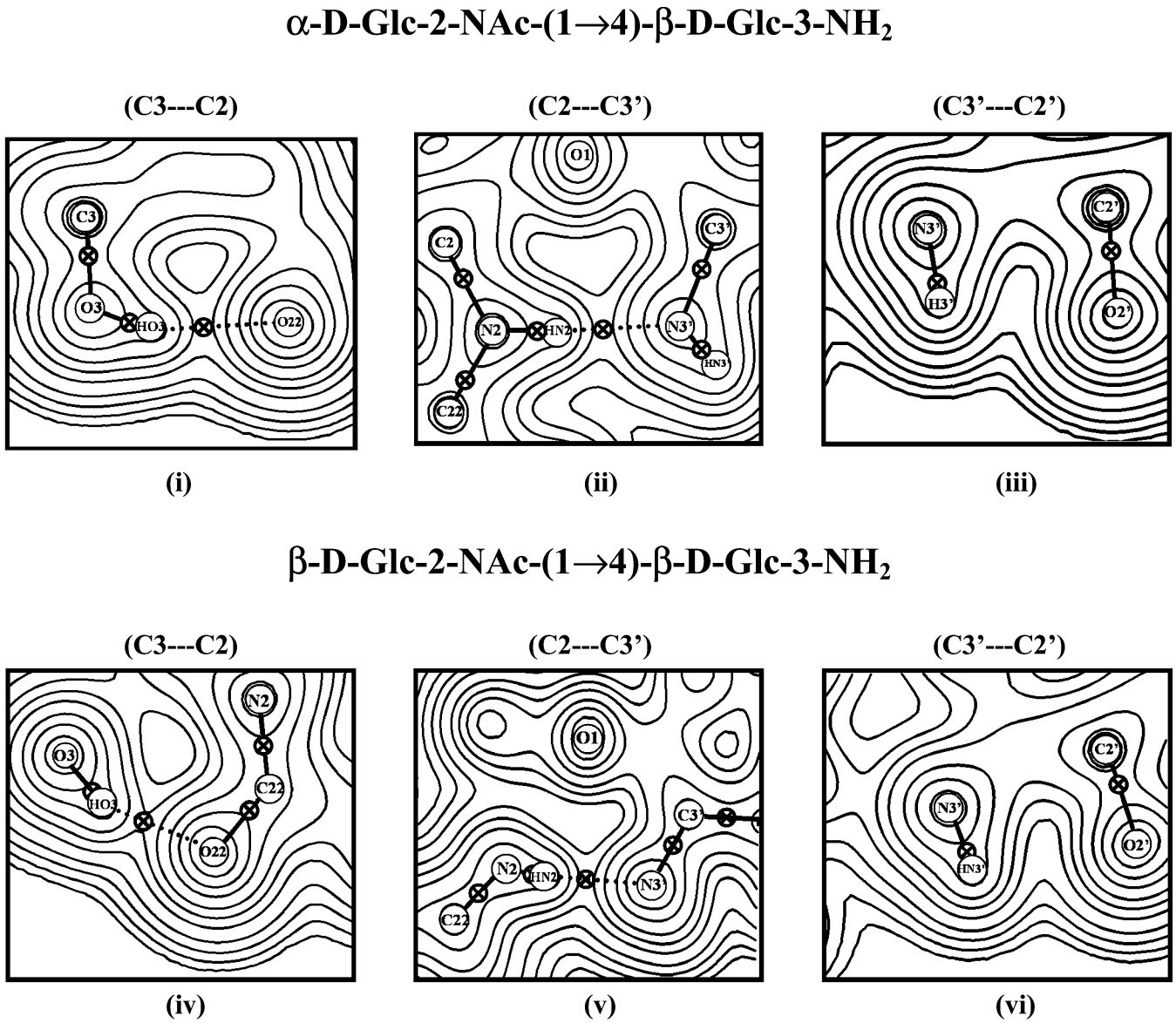

Figure 5. Electron density maps of the molecular fragments close to and about the glycosidic linkage of α-D-Glc-2-NAc−(1→4)-*β*-D-Glc-3-NH_2 (i)−(iii) and *β*-D-Glc-2-NAc−(1→4)-*β*-D-Glc-3-NH_2 (iv)−(vi)**.** The positions of the nuclei (as labeled in Figure 1) are marked with an open circle and the positions of the BCPs are marked with "⊗".

be obtained from the binding energy of model compounds. This, however, did not account for the very different conformational, structural, and chemical environments found when the functional group pairs were connected in a bonded arrangement.

We have found that intramolecular hydrogen bond strengths can be estimated by establishing a relationship between hydrogen bond energy and the topological properties of electron density between the complex. This relationship allows for the construction of correlation ΔE^{HB} vs Δ_{el+lap} curves for each combination of hydrogen bond pair. Once the ΔE^{HB} vs Δ_{el+lap} curve is constructed for a pair of hydrogen-bonded functional groups, it can be used to estimate the intramolecular hydrogen bonds for the same pair in any system. We have used these curves to estimate the cross glycosidic linkage hydrogen bond strength in (1−4) linked disaccharide derivatives and found the relative strengths of these intramolecular hydrogen bonds within their biomolecular conformational context, thereby demonstrating that a ranking of the relative intramolecular hydrogen bond strength occurring across the (1−4) glycosidic linkage is now possible. We have seen that the strongest intermolecular hydrogen bonds (e.g., Me−NH_2(A)- - -Me−OH(D)) do not result in the strongest cross-glycosidic intramolecular hydrogen bonds when the either of the hydroxyl groups at C(2) and C(3′) is substituted with an amine. This is because the hydrogen bonds between vicinal groups on the reducing and nonreducing sugars affect the formation of the cross glycosidic hydrogen bonds. Nonetheless, our estimations of intramolecular cross-glycosidic linkage hydrogen bonds showed that the NAc(D)- - -NH_2(A) hydrogen bond in α-D-Glc-2-NH_2-(1→4)-*β*-D-Glc and *β*-D-Glc-2-NH_2-(1→4)-*β*-D-Glc is stronger than OH(D)- - -OH(A) found in maltose and cellobiose.

Acknowledgment. J.Y.-J.C. thanks the National Research Foundation (NRF Pretoria) for doctoral support.

References and Notes

(1) Baker, E. L.; Hubbard, R. E. *Prog. Biophys. Mol. Biol.* **1984**, *44*, 97−179.

(2) (a) Rees, D. A. *Polysaccharide Shapes*; Chapman and Hall Ltd.: New York, 1977. (b) Atkins, E. D. T. *Polysaccharides: Topics in structure and morphology*; The Macmillan Press ltd: New York, 1985. (c) Atkins, E. D. T. In *Xylans and Xylanases*; Visser, J., Ed.; Elsevier: London, 1992; Vol. 7, pp 39−50.

(3) (a) Johnson, L. N.; Cheetham, J.; McLaughlin, P. J.; Acharya, K. R. In *Current topics in microbiology and immunology*; Clarke, A. E., Wilson, I. A., Eds.: New York, 1988; Vol. 139, pp 81−133. (b) Sharon, N.; Lis, H. *Sci. Am.* **1993**, 82−89. (c) Homans, S. W. In *Molecular glycobiology*; Fakuda, M., Hindsgaul, O., Eds.: New York, 1994; pp 231−257.

(4) (a) Dingley, A. J.; Grzesiek, S. *J. Am. Chem. Soc.* **1998**, *120*, 8293−8297. (b) Gemmecker, G. *Angew. Chem., Int. Ed.* **2000**, *39*, 1224−1226. (c) Landersjo, C.; Hoog, C.; Maliniak, A.; Widmalm, G. *J. Phys. Chem. B* **2000**, *104*, 5618−5624. (d) Hawley, J.; Bampos, N.; Aboitiz, N.; Jimenez-Barbero, J.; Lopez De la Paz, M.; Sanders, J. K. M.; Carmona, P.; Vicent, C. *Eur. J. Org. Chem.* **2002**, *12*, 1925−1936.

(5) (a) Smith, B. J.; Swanton, D. J.; Pople, J. A.; Schaefer, H. F. I.; Radom, L. *J. Chem. Phys.* **1990**, *92*, 1240−1247. (b) Gordon, M. S.; Jensen, J. H. *Acc. Chem. Res.* **1996**, *29*, 536−543.

(6) Kim, K.; Friesner, R. A. *J. Am. Chem. Soc.* **1997**, *119*, 12952−12961.

(7) Vargas, R.; Garza, J.; Friesner, R. A.; Stern, H.; Hay, B. P.; Dixon, D. A. *J. Phys. Chem. A* **2001**, *105*, 4963−4968.

(8) Pacios, L. F.; Gómez, P. C. *J. Comput. Chem* **2001**, *22*, 702−716.

(9) (a) Brady, J. W.; Schmidt, R. K. *J. Phys. Chem.* **1993**, *97*, 958−966. (b) Naidoo, K. J.; Denysyk, D.; Brady, J. W. *Protein Eng.* **1997**, *10*, 1249−1261. (c) Clarke, C.; Woods, R. J.; Gluska, J.; Cooper, A.; Nutley, M. A.; Boons, G. *J. Am. Chem. Soc.* **2001**, *123*, 12238−12247.

(10) Naidoo, K. J.; Brady, J. W. *J. Am. Chem. Soc.* **1999**, *121*, 2244−2252.

(11) Naidoo, K. J.; Kuttel, M. M. *J. Comput. Chem.* **2001**, *22*, 445−456.

(12) Naidoo, K. J.; Chen, Y. J. In *Abstr. Pap. − Am. Chem. Soc*; Witczak, Z. J., Ed.; American Chemical Society: Chicago, 2001; Vol. 222, pp CARB-119.

(13) Del Bene, J. E. *Hydrogen Bonding 1: Encyclopedia of computational chemistry*, 1st ed.; John Wiley & Sons: New York, 1998; Vol. 2.

(14) Becke, A. D. *J. Chem. Phys.* **1993**, *98*, 5648−5652.

(15) Gálvez, O.; GóMez, P. C.; Pacios, L. F *J. Chem. Phys.* **2001**, *115*, 11166−11183.

(16) Jerziorski, B.; Kolos, W. In *Molecular Interactions*; Ratajczak, H., Orville-Thomas, W. J., Eds.; Wiley: New York, 1982; Vol. 2, pp 1−46.

(17) Morokuma, K. *Acc. Chem. Res.* **1977**, *10*, 294−300.

(18) Scheiner, S. In *Reviews in Computational Chemistry*; Lipkowitz, K. B., Boyd, D. B., Eds.; VCH Publishers, Inc.: New York, 1991; Vol. 2, pp 165−218.

(19) Morokuma, K.; Kitaura, K. In *Chemical Applications of Atomic and Molecular Electrostatic Potentials*; Politzer, P., Truhlar, D. G., Eds.; Plenum: New York, 1981; pp 215−242.

(20) Bader. *Atoms in Molecues- A Quantum Theory*; Oxford University Press: Oxford, U.K., 1990.

(21) Popelier, P. L. A. *J. Phys. Chem. A* **1999**, *103*, 2883−2890.

(22) Koch, U.; Popelier, P. L. A. *J. Phys. Chem.* **1995**, *99*, 7−9754.

(23) Lipkowski, P.; Koll, A.; Karpfen, A.; Wolschann, P. *Chem. Phys. Lett.* **2002**, *360*, 256−263.

(24) Wojtulewskia, S.; Grabowski, S. J. *J. Mol. Struct. (THEOCHEM)* **2003**, *645*, 287−294.

(25) Grabowski, S. J. *J. Phys. Chem. A* **2001**, *105*, 10739−10746.

(26) Frisch, M. J.; Trucks, G. W.; Schlegel, H. B.; Scuseria, G. E.; Robb, M. A.; Cheeseman, J. R.; Montgomery, J. A.; Stratmann, R. E.; Burant, J. C.; Dapprich, S.; Millam, J. M.; Daniels, A. D.; Kudin, K. N.; Strain, M. C.; Farkas, O.; Tomasi, J.; Barone, V.; Cossi, M.; Cammi, R.; Mennucci, B.; Pomelli, C.; Adamo, C.; Clifford, S.; Ochterski, J.; Peterssin, G. A.; Al-Laham, M. A.; Zakrzewski, V. G.; Cui, Q.; Morokuma, K.; Malick, D. K.; Rabuck, A. D.; Raghavachari, K.; Goresman, J. B.; Ortiz, J. V.; Cioslowski, J.; Baboul, A. G.; Liu, G.; Liashenko, A.; Piskorz, P.; Komaromi, I.; Martin, R. L.; Fox, D. J.; Keith, T.; Gill, P. M. W.; Nanayakkara, A.; Challacombe, M.; Peng, C. Y.; Ayala, P. Y.; Chen, W.; Wong, M. W.; Johnson, B. G.; Stefanov, B. B.; Gomperts, R.; Head-Gordon, M.; Gonzalez, C.; Pople, J. A. *Gaussian98*, version A.7; Gaussian, Inc.: Pittsburgh, PA, 1998.

(27) Rablen, P. R.; Lockman, J. W.; Jorgensen, W. L. *J. Phys. Chem. A* **1998**, *102*, 3782−3797.

(28) Boys, S. F.; Bernardi, F. *Mol. Phys.* **1970**, *19*, 553−566.

(29) Biegler-König, F.; Schönbohm, J.; Bayles, D. *J. Comput. Chem* **2001**, *22*, 545−559.

(30) Martínez, A. G.; Vilar, E. T.; Fraile, A. G.; Martínez-Ruiz, P. *J. Phys. Chem. A* **2002**, *106*, 4942−4950.

(31) Del Bene, J. *J. Chem. Phys.* **1971**, *55*, 4633−4636.

(32) Dixon, J. R.; George, W. O.; Hossain, M. F.; R., L.; Price, J. M. *J. Chem. Soc., Faraday Trans.* **1997**, *93*, 3611−3618.

(33) (a) Karpen, A.; Schuster, P. *Can. J. Chem.* **1985**, *63*, 809−815. (b) Bakó, I. P., G *J. Mol. Struct. (THEOCHEM)* **2002**, *594*, 197−184. (c) González, L.; Mó, O.; Yánez, M. *J. Chem. Phys.* **1998**, *109*, 139−150. (d) Masella, M.; Flament, J. P. *J. Chem. Phys.* **1998**, *108*, 7141−7151. (e) Sum, a. K.; Sandler, S. I. *J. Phys. Chem. A* **2000**, *104*, 1121−1129. (f) Cabalerio-Lago, E. M.; Rodríguez-Otero, J. *THEOCHEM* **2002**, *586*, 225−234. (g) Kang, Y. K. *J. Phys. Chem. B* **2000**, *104*, 8321−8326. (h) Torii, H.; Tasumi, T.; Kanazawa, T.; Tasumi, M. *J. Phys. Chem. B* **1998**, *102*, 309−314.

(34) Hagemeister, F. C.; Gruenloh, C. J.; Zwier, T. S. *J. Phys. Chem. A* **1998**, *102*, 82−94.

(35) Bizzarri, A.; Stolte, S.; Reuss, J.; Van Duijneveldt-Van-de-Rijdt, J. G. C. M.; Van Duijneveldt, F. B. V. *Chem. Phys.* **1990**, *143*, 423−435.

(36) Tatamitani, Y.; Liu, B.; Shimada, J.; Ogata, T.; Ottaviani, P.; Maris, A.; Caminati, W.; Alonso, J. L. *J. Am. Chem. Soc.* **2002**, *124*, 2739−2743.

(37) Cheeseman, J. R.; Carroll, M. T.; Bader, R. F. W. *Chem. Phys. Lett.* **1998**, *143*, 450−458.

(38) (a)Taylor, R.; Kennard, O.; Versichel, W. *J. Am. Chem. Soc.* **1983**, *105*, 5761−5766. (b)Taylor, B.; Kennard, O.; Versichel, W. *Acta Crystallogr.* **1984**, *B40*, 280−288. (c)Murray-Rust, P.; Glusker, J. P. *J. Am. Chem. Soc.* **1984**, *106*, 1018−1025.

(39) Adalsteinsson, H.; Maultiz, A. H.; Bruice, T. C. *J. Am. Chem. Soc.* **1996**, *118*, 7689−7693.

(40) (a) Coulson, C. A.; Danielson, U. *Ark. Fys.* **1954**, *8*, 239−244. (b) Coulson, C. A.; Danielson, U. *Ark. Fys.* **1954**, *8*, 245−255. (c) Tsubomura, H. *Bull. Chem. Soc. Jpn.* **1954**, *27*, 445−450.

(41) Best, R. E.; Jackson, G. E.; Naidoo, K. J. *J. Phys. Chem. B* **2001**, *105*, 4742−4751.

(42) Klein, R. A. *J. Comput. Chem.* **2002**, *23*, 585−599.